Chapter 10
Development of a Novel Robotic Continuously Scanning Laser Doppler Vibrometer for Vibration Measurement of a Beam

Ke Yuan and Weidong Zhu

Abstract A continuously scanning laser Doppler vibrometer (CSLDV) has been widely used to measure structural vibrations due to its high measurement efficiency and spatial resolution. However, a conventional CSLDV, which conducts continuous scanning through two rotating scan mirrors, is limited by its field of view. This work proposes a novel robotic CSLDV system that combines a robotic arm and a laser vibrometer to provide a more flexible approach to obtaining modal parameters of a structure. A central control and data acquisition system is developed to synchronously control the robotic arm, laser vibrometer, and excitation device during the measurement. A new signal processing method is developed to separate vibration signals of the structure from motion signals of the laser vibrometer in the measured response, and to extract mode shapes of the structure. The proposed system and signal processing method are experimentally validated by identifying the first mode shape of a beam under sinusoidal excitation. Mode shapes measured using the conventional CSLDV and the proposed system in a point-by-point manner are used as references. Modal Assurance Criterion values among mode shapes from the three experiments are greater than 99%.

Keywords Laser Doppler vibrometry · CSLDV · robot-assisted vibration measurement · modal identification· signal processing

Introduction

As an optical-based device, the continuously scanning laser Doppler vibrometer (CSLDV) has a limited field of view (FOV) and cannot measure vibrations in areas outside of it. Various studies have been conducted to develop advanced measurement methodologies to extend the FOV of the laser vibrometer. Two common methods are moving the laser vibrometer to different positions [1] and using a reflective mirror to redirect the laser beam of the laser vibrometer [2, 3, 4]. The first method involves building a global coordinate system using reference objects and reconstructing vibrations of different areas based on that system. However, measurement errors can be introduced during the repositioning of the device, and the method becomes less feasible as the number of measurement surfaces increases due to strict experimental setup requirements. The second method keeps positions of both the laser vibrometer and the test structure unchanged to minimize movement errors, redirecting the laser beam to otherwise unmeasurable areas via reflective mirrors. Yuan and Zhu [3] developed a novel mirror-assisted testing methodology, including a new algorithm to design continuous and synchronous scan trajectories using mirrored areas, and a new signal processing method that stitches vibration signals from different parts of the structure using mirrored laser heads for three-dimensional (3D) CSLDV measurements. Although this method supports measurements of structures with complex surfaces, such as cylindrical ones, it requires mirrors of appropriate sizes and carefully placed orientations, which can significantly increase experimental duration.

Ke Yuan
Michael W. Hall School of Mechanical Engineering Mississippi State University, Mississippi State, MS 39762
e-mail: ky309@msstate.edu

Weidong Zhu
Department of Mechanical Engineering
University of Maryland Baltimore County, Baltimore, MD 21250
e-mail: wzhu@umbc.edu

© The Author(s), under exclusive license to River Publishers 2026

Kristin B. Zimmerman, PhD (eds.), *Computer Vision and SLDV for Structural Dynamics, 2026, Vol. 6*, Conference Proceedings of the Society for Experimental Mechanics Series, https://doi.org/10.13052/rp-9788743814177

Using robotic platforms such as unmanned aerial vehicles (UAVs) or robotic arms to assist structural health monitoring has received growing attention due to the increased flexibility and accessibility they provide. For example, UAV-assisted crack detection methods have been developed using image processing techniques for bridges with ongoing traffic [5]. UAV-based digital image correlation systems [6, 7] have also been developed to capture dynamic responses of large infrastructures. Mounting a laser vibrometer on a programmable moving platform like a UAV or robotic arm offers a promising approach to overcoming limitations of traditional vibration measurement systems. By inputting programmed positions and orientations into the UAV or the robotic arm, the laser spot can be directed accurately to desired positions on the structure, avoiding manual movement errors. Refs. [8, 9] proposed UAV+LDV solutions and developed correction methods to compensate for angular and linear movement errors. Other studies [10, 11, 12, 13, 14, 15] demonstrated the application of robot+LDV systems for vibration measurements in industrial scenarios, such as damage detection in composite plates and model updating of bladed wheels. In these studies, large industrial robotic arms were often used to accommodate multiple laser heads for full-field 3D vibration measurements, which increased space and cost requirements. In Ref. [16], a 3D robot+LDV system using only one laser head was proposed to reduce the payload requirement of the robotic arm to 3 kg, making the system more compact and suitable for laboratory environments. However, existing robot-assisted LDV systems have primarily focused on step-by-step measurements, and there is a lack of studies on integrating robotic arms with the CSLDV technique to significantly increase measurement efficiency. For instance, authors of Ref. [16] reported that their approach required approximately 20 hours to test 301 measurement points, since additional time was needed for the robotic arm to reposition sequentially among target points. Moreover, the contribution of the robotic motion itself was neglected in their analysis, which may limit both measurement efficiency and accuracy.

The first contribution of this work is the development of a novel robotic CSLDV system for structural vibration measurement. The proposed system consists of a six-axis robotic arm and a compact laser vibrometer. The major difference between the proposed robotic CSLDV system and the conventional CSLDV lies in the scanning mechanism: in the conventional CSLDV, the laser head is stationary and the laser spot moves via rotating scan mirrors, whereas in the robotic CSLDV system, the laser head and the laser spot move together through joint rotations of the robotic arm. Previous research [17, 18, 19] has shown that speckle noise is a major factor affecting the quality of vibration measurements using moving laser vibrometers. In this work, a chip-based laser vibrometer with real-time speckle compensation [20] is used to obtain vibration responses with reduced noise and improved quality. The second contribution of this work is the development of a novel notch-filter-enhanced demodulation (NFED) method to identify modal parameters of structures under sinusoidal excitation. The conventional demodulation method for conventional CSLDV measurements has limited accuracy when applied to signals from the proposed robotic CSLDV system, due to low-frequency interference introduced by the motion of the laser head. The proposed NFED method can separate vibration signals of a structure from motion signals of the laser vibrometer in the measured response and extract mode shapes of the structure. The proposed system and signal processing method are experimentally validated by identifying the first mode shape of a beam under sinusoidal excitation. Mode shapes measured using the conventional CSLDV and the proposed system in a point-by-point manner are used as references. Modal Assurance Criterion (MAC) values among mode shapes from the three experiments are greater than 99%. In addition, the effect of the running speed of the proposed system on the estimated mode shape is investigated in this work. Compared to previous robot+LDV studies, the proposed robotic CSLDV system leverages continuous programmed motion of the robotic arm to achieve vibration measurements along arbitrary scan trajectories in a fraction of the time, while explicitly addressing robot-induced motion effects through the proposed NFED signal processing method.

Methodology

As shown in Figure 1a, the proposed system consists of a compact laser vibrometer and a six-axis robotic arm, which are connected via an adapter. Six joints of the robotic arm, from its base to its tip, are denoted as J1-J6, and and each can be independently controlled by an internal motor. During vibration measurement, the movement of the robotic arm, DAQ of the laser vibrometer, and excitation provided by a modal shaker are synchronized by a central control and DAQ system, as shown in Figure 1b.

The working principle of the central control and DAQ system via Simulink is illustrated in Figure 2a. The control model consists of three tracks corresponding to the modal shaker, the laser vibrometer, and the robotic arm, respectively. Initial signals for the three blocks denoting shaker switch, laser trigger, and robot trigger, respectively, are all set to zero, and digital signals are applied to initiate vibration measurements. The gain blocks of 0.1 are used as required scalings in the model because a value of 1 V in a digital-to-analog converter (DAC) corresponds to an output of 10 V. Figure 2b provides an example of digital signals used during testing. In the top track, the modal shaker is controlled by a switch block. Its data inputs, shown in the first and third ports, are a series of excitation and zero signals, respectively. The control input, shown in

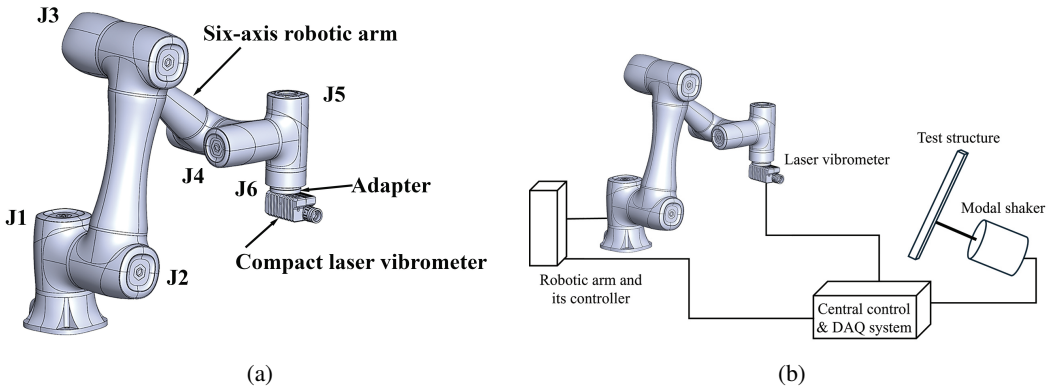

(a) (b)

Fig. 1 (a) Proposed novel robotic CSLDV system, consisting of a six-axis robotic arm and a compact laser vibrometer, and (b) the working principle of the robotic CSLDV system, where the robotic arm, the laser vibrometer, and the modal shaker are synchronized by a central control and DAQ system

the second port, has a threshold value of zero. Data are sent to the modal shaker via the DAC, shown at the right end of the top track. The saturation block in the top track is used for limiting the range of signals to avoid undesired sensor overload. From Figure 2b, the control input consists of two phases: a waiting time and a testing time. During the waiting time, the control input signal remains zero, which does not meet the threshold; therefore, the switch block passes zero signals, and the modal shaker remains disabled. At the end of the waiting time, which is 3 seconds in this example, the signal value switches to one, meeting the threshold. As a result, the switch block passes excitation signals, which are chirp signals in this example, and the modal shaker is activated. The middle and bottom tracks in Figure 2a show triggers for DAQ of the laser vibrometer and the movement of the robotic arm, respectively. Both tracks follow similar logic: a digital pulse is used as the trigger signal near the start of the testing time. The only difference is that the laser vibrometer is triggered by the falling edge of the pulse, while the robotic arm is triggered by the rising edge.

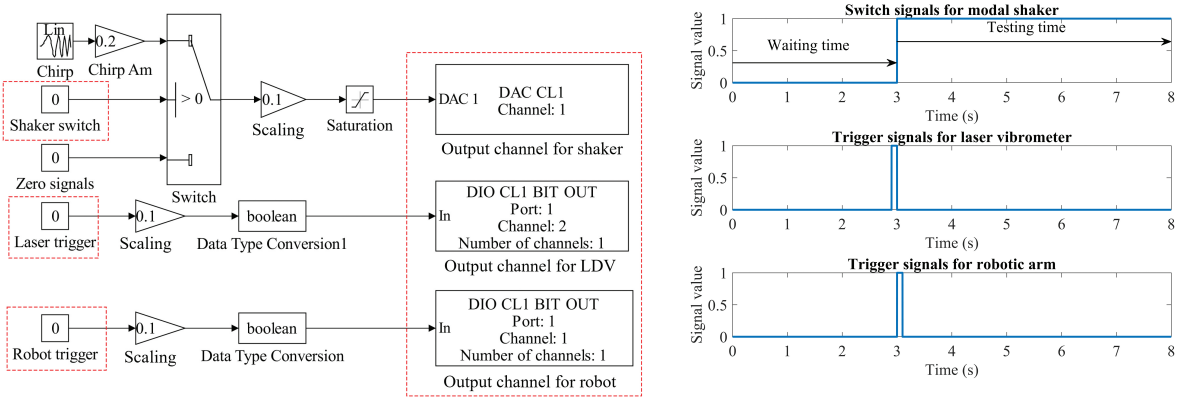

(a) (b)

Fig. 2 (a) Working principle of the central control and DAQ system, and (b) switch and trigger signals for the modal shaker, the laser vibrometer, and the robotic arm, used to synchronously control all three components

Continuous scanning measurements can be performed using the proposed system by continuously moving the laser vibrometer. This approach is significantly different from a conventional CSLDV system, which performs continuous scanning by rotating a pair of orthogonal scan mirrors. An example of using the proposed robotic CSLDV system to scan a beam-like structure is shown in Figure 3a, where the laser vibrometer is translated along a straight line on the surface of the beam at a constant speed. A complete scan in this study is defined as the laser spot moving from the start point to the end point and then returning. The period of one scan is denoted as T, and the scan frequency is given by $f_{sc} = 1/T$. The distance between the laser head and the surface of the test beam remains constant during scanning, indicating that the tool center point (TCP) of the system follows a linear trajectory.

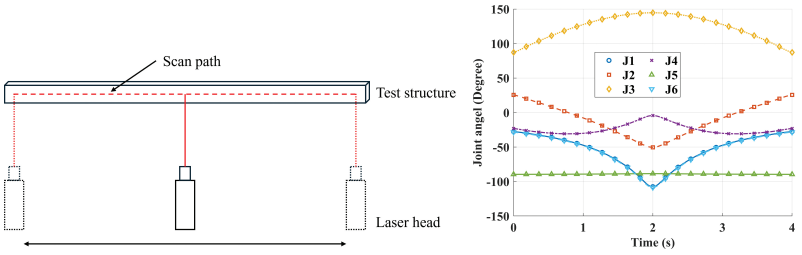

(a) (b)

Fig. 3 (a) An example of a scan path executed by the proposed system along a straight line on the surface of a beam, and (b) time series of rotation angles of robotic arm joints J1-J6 corresponding to the straight-line path

Kinematics of the proposed robotic CSLDV system can be described using the Denavit–Hartenberg (DH) convention [21],

$$ {}^{0}_{la}T = T_1^0 T_2^1 T_3^2 T_4^3 T_5^4 T_6^5 T_{la}^6 \tag{1} $$

where ${}^{0}_{la}T$ denotes the transformation matrix describing the pose of the laser spot, which is an end-effector in this work, relative to the base of the system, T_i^{i-1} denotes the relative pose of the ith joint to the $(i-1)^{\text{th}}$ joint, and T_{la}^6 represents the pose of the laser spot relative to joint J6. Each T_i^{i-1} is determined by DH parameters, including link lengths a, link offsets d, link twists α, and joint angles θ. The first three parameters are known from the robotic arm's physical configuration. T_{la}^6 can be determined from the laser head geometry and its distance to the test structure. Inverse kinematics (IK) based on DH parameters of the system is used to calculate its joint angles θ as

$$ \theta_i = f^{-1}({}^{0}_{la}P) \tag{2} $$

where ${}^{0}_{la}P$ denotes the position of the laser spot in the base coordinate system.

In this work, a commercial Collaborative robot (Cobot) model DOBOT CR5A (Shenzhen Dobot Corp Ltd) and its control software, DobotStudio, are used to solve the IK equations and obtain joint angles. As a Cobot, the CR5A allows teaching by manually guiding the end-effector to the desired start and end points of the scan path in drag mode. These positions are recorded and used as input parameters for the IK. The joint rotation angles for a straight-line path at $f_{sc} = 0.25$ Hz are shown in Figure 3b. The joint J6 exhibits the largest rotation of 80.1 degrees from start to end, while the joint J5 rotates by only 1 degree. To maintain a constant TCP speed, each joint rotates at a different rate.

The response of the beam without excitation, as shown in Figure 4a, is measured using the displacement-based laser vibrometer in the proposed system to verify the scan path. The measured response has an amplitude of less than 0.8 mm, as indicated by the dashed lines, suggesting that the distance between the start and end points is also less than 0.8 mm. Given the beam length of 548 mm, the angle error between the actual and designed scan paths is approximately 0.08 degrees, indicating high accuracy in laser spot positioning. The response of the beam under sinusoidal excitation at 66.67 Hz, which is close to the first natural frequency of the beam, is shown in Figure 4b. The system captures both the low-frequency motion of the laser head and the high-frequency vibration of the beam, demonstrating an advantage of the displacement-based laser vibrometer over conventional velocity-based models.

In conventional CSLDV measurements, the output response of a structure is a vibration signal modulated by spatial deflection due to continuous scanning motion [22]. When a straight-line scan trajectory is used to direct the laser spot across the structure, the response distribution $u(x,t)$ can be expressed as

$$ u(x,t) = U_I(x)\cos(\omega_e t) + U_Q(x)\sin(\omega_e t) \tag{3} $$

where $U_I(x)$ and $U_Q(x)$ represent in-phase (real) and the quadrature (imaginary) components of the mode shape of the structure, ω_e is the excitation frequency, and x denotes the spatial coordinate along the scan path, normalized within [-1,1]. For a CSLDV measurement with a uniform scanning rate, in which $x = f(t)$, this spatially varying response can be expressed purely as a function of time [23]:

$$ u(t) = u_I(t)\cos\omega_e t + u_Q(t)\sin\omega_e t \tag{4} $$

To extract u_I and u_Q, the response is multiplied by cosine and sine functions of the excitation frequency, yielding:

$$ \begin{aligned} u(t)\cos\omega_e t &= u_I(t)\cos^2\omega_e t + u_Q(t)\sin\omega_e t\cos\omega_e t \\ &= \frac{1}{2}u_I(t) + \frac{1}{2}u_I(t)\cos 2\omega_e t + \frac{1}{2}u_Q(t)\sin 2\omega_e t \end{aligned} \tag{5} $$

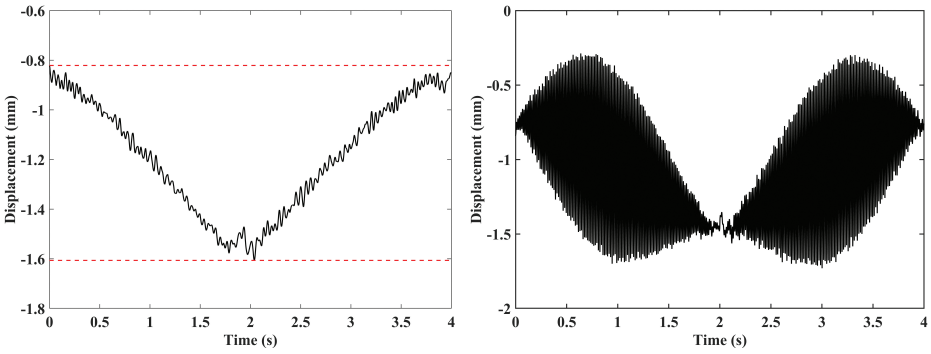

(a) (b)

Fig. 4 Measured responses of the beam: (a) without excitation, and (b) under sinusoidal excitation at 66.67 Hz

$$\begin{aligned} u(t)\sin\omega_e t &= u_I(t)\cos\omega_e t\sin\omega_e t + u_Q(t)\sin^2\omega_e t \\ &= \frac{1}{2}u_Q(t) + \frac{1}{2}u_I(t)\sin 2\omega_e t - \frac{1}{2}u_Q(t)\cos 2\omega_e t \end{aligned} \tag{6}$$

Signal components with frequency $2\omega_e$ can be removed by applying a low-pass filter, and scaling the filtered signals by a factor of 2 yields the desired components $u_I(t)$ and $u_Q(t)$. Finally, mode shape components can be obtained by substituting $t = f^{-1}(x)$ into $u_I(t)$ and $u_Q(t)$.

This method is referred to as demodulation, as it separates the vibration signal from spatial modulation effects. To test the applicability of the demodulation method to the proposed robotic CSLDV system, it was used to process the response shown in Figure 4b. As seen in Figure 5a, the resulting first mode shape of the beam is not smooth and exhibits noticeable boundary distortions, as highlighted by dashed circles, differing significantly from results obtained using the conventional CSLDV [24]. To investigate the cause of this inaccuracy, a frequency spectrum of the measured response was obtained using a fast Fourier transform (FFT), as shown in Figure 5b. The spectrum displays two dominant peaks at 0.25 Hz and 66.67 Hz, corresponding to the laser head motion and the beam vibration, respectively. The proximity of the low-frequency motion signal to zero frequency reduces the effectiveness of the low-pass filter in the demodulation method, resulting in inaccurate mode shape identification.

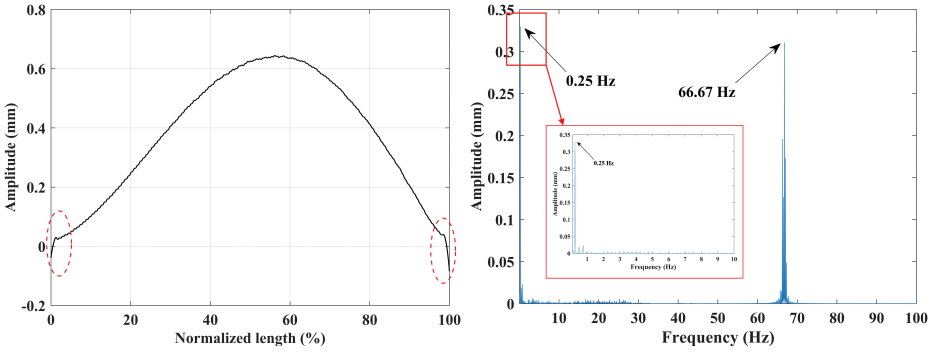

(a) (b)

Fig. 5 (a) First mode shape of the beam identified from the response shown in Figure 4b using the conventional demodulation method, and (b) the frequency spectrum of the measured response, displaying two dominant peaks at 0.25 Hz and 66.67 Hz

To overcome this limitation, a notch-filter-enhanced demodulation (NFED) method is proposed. In this method, notch filters are applied to the measured response to isolate the low-frequency laser head motion and high-frequency beam vibration. Each notch is implemented as a second-order infinite impulse response filter with complex-conjugate zeros on the unit circle at the target frequency and slightly retracted poles to set the notch selectivity. The discrete-time transfer function is

$$H(z) = \frac{1 - 2\cos(\omega_0)z^{-1} + z^{-2}}{1 - 2r\cos(\omega_0)z^{-1} + r^2 z^{-2}} \tag{7}$$

where $\omega_0 = 2\pi F_0/F_s$, F_s is the sampling rate, F_0 is the center frequency of the notch that can be set to either the scan frequency f_{sc} or the excitation frequency f_e, and $r \in (0, 1)$ is the pole radius that controls the notch bandwidth. In this work, $r = 0.99$ is used to achieve a narrow, selective notch around F_0.

To isolate the structural vibration for demodulation, the measured signal is filtered with a notch centered at f_{sc} by removing laser head motion. Conversely, to visualize the robot-motion component, a notch centered at f_e can be applied. Separated signals are shown in Figure 6a, with the top subplot showing the beam vibration and the bottom subplot showing the laser head motion. Their respective frequency spectra are provided in Figure 6b, each exhibiting a single prominent peak. With the beam vibration signal filtered, its mode shape can be accurately extracted using the demodulation method, as shown in Figure 6c.This enhancement addresses limitations of the conventional demodulation approach for the proposed robotic CSLDV system.

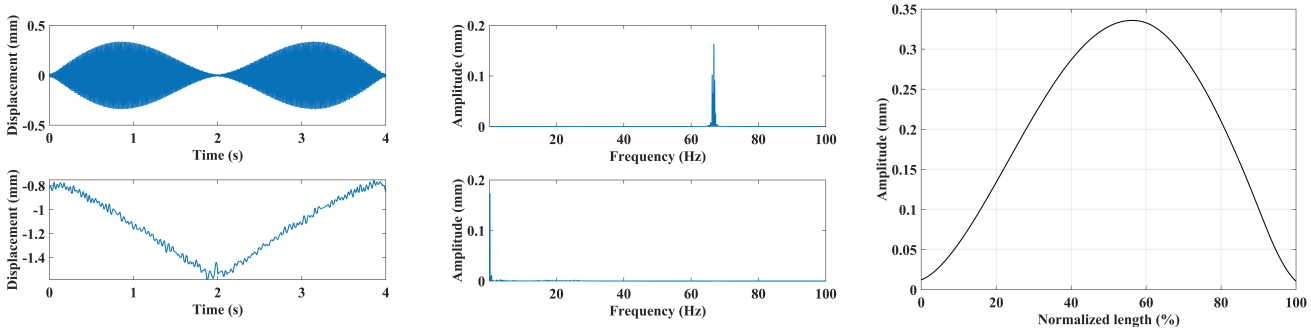

Fig. 6 Separated signals using notch filters applied to the measured response of the beam: (a) time domain and (b) frequency domain, where the top subplots show the beam vibration and the bottom subplots show the laser head motion, and (c) the first mode shape of the beam identified using the proposed NFED method

Experimental investigation

In this section, a series of experiments were conducted to validate the proposed robotic CSLDV system for modal identification of a beam under sinusoidal excitation. The experimental setup is shown in Figure 7, where Figure 7a displays the initial position of the robotic CSLDV system, and Figure 7b shows the test position. The six-axis robotic arm used in this study is the DOBOT CR5A model (Shenzhen Dobot Corp. Ltd., Shenzhen, China), and the laser vibrometer is the MotionGo model (OmniSensing Photonics LLC, Maryland, USA). A machined flange was used to connect the vibrometer to the robotic arm. The payload capacity of the CR5A is 5,000 g, while the total weight of the MotionGo vibrometer and the flange is 530 g that is well within the payload limit of the robotic arm.

In the system's initial position, where the rotation angles of all six joints are set to zero, the laser beam is parallel to the beam surface, meaning that the test beam lies outside the FOV of the system. This configuration is difficult to measure using the conventional CSLDV. The test beam is clamped at one end in a bench vise and excited at the other end using a modal shaker driven by a sinusoidal signal with a frequency of 66.67 Hz, which is close to its first natural frequency. In the test position, the laser head moves along the scan direction shown in Figure 7b, which is parallel to the beam surface. The total scan length is 548 mm, and the joint angles for this scanning motion are identical to those shown in Figure 3.

In this experiment, the running speed of the system was set to 274 mm/s, corresponding to a scan frequency of 0.25 Hz. Five complete scans, taking a total of 20 seconds, were conducted. Vibration signals of the beam, separated from the measured response using the NFED method, are shown in Figure 8a. An averaging technique was applied to the vibration signals to obtain the response from one complete scan, as shown in Figure 8b. This averaged signal was used to extract the mode shape of the beam using the proposed NFED method. In addition, two reference experiments were conducted to validate the mode shape identified by the robotic CSLDV system. The first reference experiment that can be referred to as reference 1 used the conventional CSLDV with the same scan frequency of 0.25 Hz. The second reference experiment that can be referred reference 2 used the proposed robotic CSLDV system in a point-by-point scanning mode, where the system paused at each point for measurement before moving to the next one.

Figure 8c compares the first mode shapes of the beam obtained from all three experiments, where the solid line denotes the first mode shape of the beam identified using the proposed robotic CSLDV system, the dashed line denotes that identified

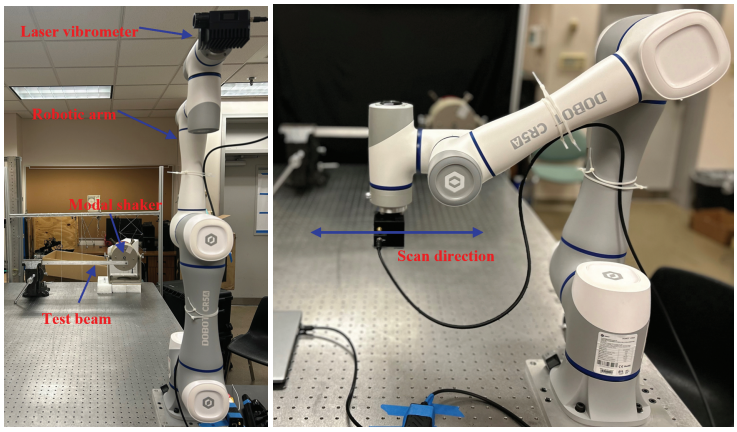

Fig. 7 (a) Experimental setup of vibration measurement of the beam using the robotic CSLDV system in its initial position, where the laser beam is parallel to the beam surface, and (b) the test position of the robotic CSLDV system, where the arrow indicates its scan direction

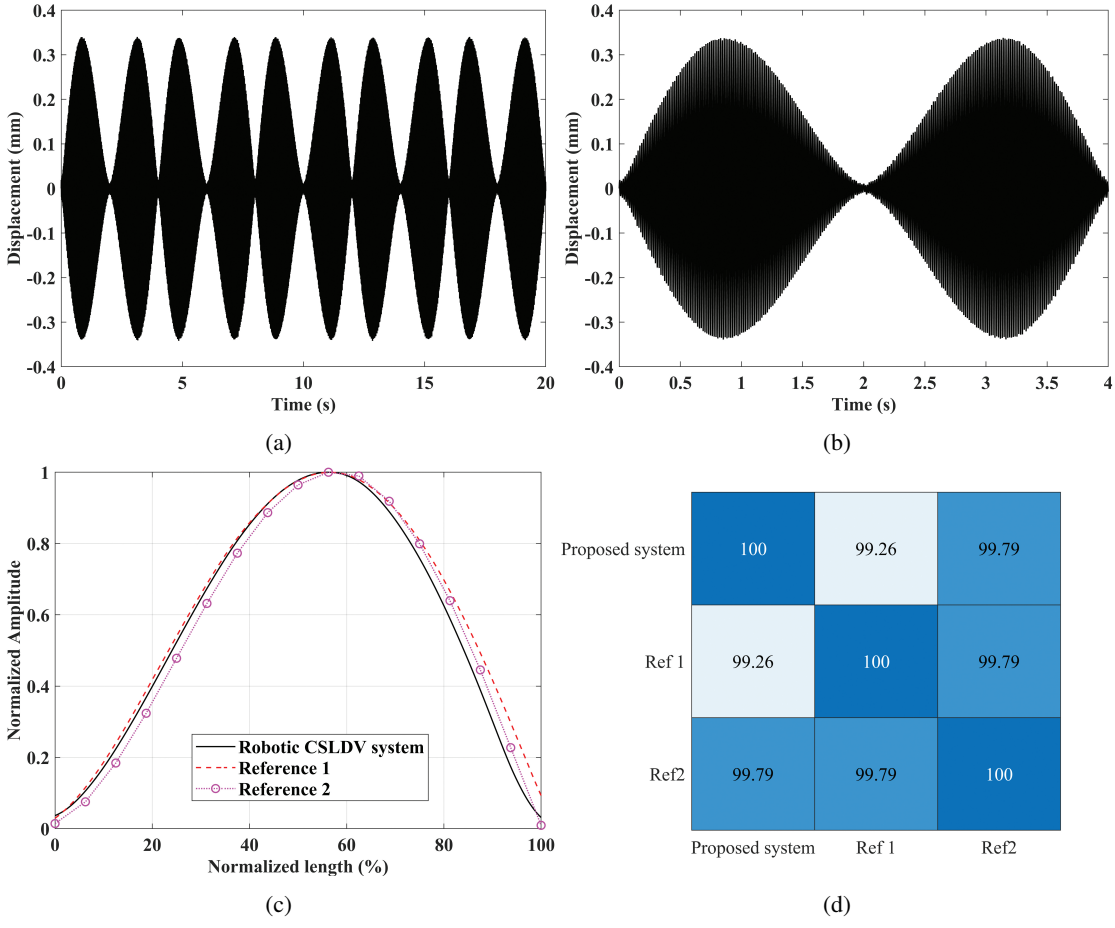

Fig. 8 (a) Vibration signals of the beam measured over five complete scans, (b) averaged vibration signal from one complete scan, used to extract the mode shape of the beam using the proposed NFED method, (c) first mode shapes of the beam identified using the proposed robotic CSLDV system, the conventional CSLDV, and the point-by-point method, and (d) MAC values among the identified mode shapes

using the conventional CSLDV, and the line with circular markers denotes that identified in the point-by-point way. The mode shape identified by the proposed system closely matches those from both reference experiments. To quantitatively evaluate the correlation among the identified mode shapes, MAC values [25] were calculated using:

$$\mathrm{MAC}(\{\varphi_r\},\{\varphi_s\}) = \frac{|\{\varphi_r\}^{\mathrm{T}}\{\varphi_s\}|^2}{(\{\varphi_r\}^{\mathrm{T}}\{\varphi_r\})(\{\varphi_s\}^{\mathrm{T}}\{\varphi_s\})} \times 100\% \tag{8}$$

where φ_r and φ_s are modal vectors of the rth and s^{th} modes of the structure, respectively, and the superscript T denotes matrix transpose. A MAC value close to 100% indicates strong correlation between two mode shapes, while a value near 0 indicates weak correlation. The resulting MAC matrix is shown in Figure 8d. The off-diagonal MAC values between the mode shape identified by the proposed system and those from the two reference experiments are both greater than 99%, confirming the high consistency among them. Comparison among test duration, number of measurement points, and availability beyond the FOV of the three measurement systems is shown in Table 1. While all three methods achieve comparable accuracy in identifying the mode shape of the beam, the proposed robotic CSLDV system offers an extended FOV compared to the conventional CSLDV and reduced test duration with higher spatial resolution compared to the point-by-point method.

Table 1 Comparison among test duration, number of measurement points, and availability beyond the FOV of the three measurement systems

System	Test duration (s)	Number of measurement points	Availability beyond the FOV
Robotic CSLDV	20	80,000	Yes
Conventional CSLDV	20	80,000	No
Single-point LDV	101	17	No

Conclusions

A novel robotic CSLDV system, which integrates a six-axis robotic arm and a compact laser vibrometer, was developed in this study to measure structural vibrations with high spatial resolution and scanning flexibility. A NFED method was proposed to separate structural vibration signals from the motion-induced components of the laser vibrometer. Experimental validation and comparative studies were carried out to assess the accuracy and repeatability of the system in identifying beam mode shapes under sinusoidal excitation. Main conclusions from this work are summarized below:

1. A robotic CSLDV system was developed to perform continuous scanning along arbitrary paths via robot arm motion, offering extended FOV compared to conventional CSLDV systems using scan mirrors.
2. A new NFED method was proposed, enabling accurate extraction of structural vibration signals even when robotic motion introduces low-frequency noise near zero frequency in the measurement signal.
3. Experimental validation confirmed high accuracy of the proposed system: the identified first mode shape of a cantilever beam matched well with reference measurements, with MAC values exceeding 99% compared to conventional CSLDV and point-by-point methods.

Acknowledgments This research was supported by the National Science Foundation through Grant No. CMMI-1763024 and the Maryland Technology Development Corporation through the Maryland Innovation Initiative Grant.

References

1. Chen, Y., Escalera Mendoza, A., and Griffith, D. "Experimental dynamic characterization of both surfaces of structures using 3d scanning laser Doppler vibrometer". *Experimental Techniques*, 47(5):989–1006 (2023).
2. Witt, B., Rohe, D., and Schoenherr, T. "Full-field strain shape estimation from 3D SLDV". In *Rotating Machinery, Optical Methods & Scanning LDV Methods, Volume 6: Proceedings of the 37th IMAC, A Conference and Exposition on Structural Dynamics 2019*, pages 31–45. Springer (2019).

3. Yuan, K. and Zhu, W. "A novel mirror-assisted method for full-field vibration measurement of a hollow cylinder using a three-dimensional continuously scanning laser Doppler vibrometer system". *Mechanical Systems and Signal Processing*, 216:111428 (2024).
4. Yuan, K., Yuan, S., and Zhu, W. "Full-field modal analysis of a tensegrity column using a three-dimensional scanning laser Doppler vibrometer with a mirror". *Journal of Vibration and Acoustics*, 146(6):061101 (2024).
5. Gadiraju, D.S., Azam, S.E., and Khazanchi, D. "Shm-traffic: DRL and transfer learning based UAV control for structural health monitoring of bridges with traffic". *IEEE Access*, 13:6166–6179 (2025).
6. Jeong, E., Seo, J., and Wacker, J. "New bridge inspection approach with joint UAV and DIC system". In *Structures Congress 2020*, pages 349–359. American Society of Civil Engineers Reston, VA (2020).
7. Lavezzi, G., Ciarcià, M., Won, K., and Tazarv, M. "A DIC-UAV based displacement measurement technique for bridge field testing". *Engineering Structures*, 308:117951 (2024).
8. Garg, P., Moreu, F., Ozdagli, A., Taha, M.R., and Mascareñas, D. "Noncontact dynamic displacement measurement of structures using a moving laser Doppler vibrometer". *Journal of Bridge Engineering*, 24(9):04019089 (2019).
9. Garg, P., Nasimi, R., Ozdagli, A., Zhang, S., Mascarenas, D.D.L., Reda Taha, M., and Moreu, F. "Measuring transverse displacements using unmanned aerial systems laser Doppler vibrometer (UAS-LDV): Development and field validation". *Sensors*, 20(21):6051 (2020).
10. Oliver, D.E., Schuessler, M., et al. "Automated robot-based 3D vibration measurement system". *Sound Vib*, 43:12–15 (2009).
11. Ziemer, T. and Rembe, C. "Demonstration of a 3D vibration measurement with a single-point laser Doppler vibrometer and a 6-axis industrial robot". In *Proceedings of the International Symposium on Optoelectronic Technology 2016*, pages 1–10 (2016).
12. Bertini, L., Neri, P., Santus, C., and Guglielmo, A. "Automated experimental modal analysis of bladed wheels with an anthropomorphic robotic station". *Experimental Mechanics*, 57:273–285 (2017).
13. Devigne, O., Hoffait, S., and Bruls, O. "Development of a robot-aided modal analysis measurement method using laser Doppler vibrometry". In *ISMA 2020 (29th Leuven Conference on Noise and Vibration Engineering)*, pages 1847—-1858 (2020).
14. Ahmed, H., Mohsin, A., Hong, S.C., Lee, J.R., and Ihn, J.B. "Robotic laser sensing and laser mirror excitation for pulse-echo scanning inspection of fixed composite structures with non-planar geometries". *Measurement*, 176:109109 (2021).
15. Brethee, K.F., Uwayed, A.N., and Alden Qwam, A.Y. "A novel index for vibration-based damage detection technique in laminated composite plates under forced vibrations: Experimental study". *Structural Health Monitoring*, 22(5):3109–3125 (2023).
16. Margerit, P., Gobin, T., Lebée, A., and Caron, J.F. "The robotized laser Doppler vibrometer: On the use of an industrial robot arm to perform 3D full-field velocity measurements". *Optics and Lasers in Engineering*, 137:106363 (2021).
17. Bendel, K., Fischer, M., and Schuessler, M. "Vibrational analysis of power tools using a novel three-dimensional scanning vibrometer". In *Sixth international conference on vibration measurements by laser techniques: advances and applications*, volume 5503, pages 177–184. SPIE (2004).
18. Sels, S., Vanlanduit, S., Bogaerts, B., and Penne, R. "Three-dimensional full-field vibration measurements using a handheld single-point laser doppler vibrometer". *Mechanical Systems and Signal Processing*, 126:427–438 (2019).
19. Zeng, Y., Nunez, A., and Li, Z. "Speckle noise reduction for structural vibration measurement with laser Doppler vibrometer on moving platform". *Mechanical Systems and Signal Processing*, 178:109196 (2022).
20. Yuan, K., Zhu, Z., Chen, W., and Zhu, W. "Development and validation of a new type of displacement-based miniatured laser vibrometers". *Sensors*, 24(16):5230 (2024).
21. Denavit, J. and Hartenberg, R.S. "A kinematic notation for lower-pair mechanisms based on matrices". *Journal of Applied Mechanics*, 22(2):215–221 (2021).
22. Sriram, P., Hanagud, S., and Craig, J. "Mode shape measurement using a scanning laser Doppler vibrometer". *The International Journal of Analytical and Experimental Modal Analysis*, 7(3):169–178 (1992).
23. Stanbridge, A. and Ewins, D. "Modal testing using a scanning laser Doppler vibrometer". *Mechanical Systems and Signal Processing*, 13(2):255–270 (1999).
24. Chen, D.M., Xu, Y., and Zhu, W. "Experimental investigation of notch-type damage identification with a curvature-based method by using a continuously scanning laser Doppler vibrometer system". *Journal of Nondestructive Evaluation*, 36(2):38 (2017).
25. Ewins, D. *Modal Testing: Theory, Practice and Application*. Engineering dynamics series. Wiley (2000).